Parameterization of momentum flux and energy flux associated with orographically excited internal gravity waves in a baroclinic background flow

SOMENATH DUTTA

Meteorological Office, Pune, India

(*Received 18 July 2006, Modified 21 February 2007*)

e mail : duttapne@yahoo.co.in

सार – इस षोध पत्र में त्रि–आयामी मध्य मापक्रम दीर्घवृत्ताकार घेरे के आर–पार वायु प्रवाह के ऊर्ध्वाधर ऊर्जा फलक्स (E_z) तथा संवेग फलक्स (τ_{zx} और τ_{zy}) के क्षैतिज अवयवों जिनकी आंतरिक गुरूत्व तरंगे पर्वतीय क्षेत्र में दाब प्रवणिक पृष्ठ भूमि बहाव की तरफ निर्गमन करती हैं, को प्राचलीकृत करने के लिए एक रैखिक गत्यात्मक मॉडल का प्रयोग किया गया है। इस मॉडल का प्रयोग असमान पर्वतीय क्षेत्र के अवरोधक के लिए किया जा सकता है, यद्यपि इस षोध पत्र में एक दीर्घवृत्ताकार अवरोधक की धारणा पर विचार किया गया है। इस मॉडल में स्थायित्व के लिए वास्ताविक ऊर्ध्वाधर भिन्नताओं को संयुक्त किया गया है। इस मॉडल की उत्पत्ति कुछ चुने हुए भारतीय पर्वतों (पष्चिमी घाट की पहाड़ियों और खासी जयंतिया पहाड़ियों) पर प्राप्त किए गए अर्द्ध संख्यात्मक आंकड़ों के आधार पर हुई है।

(*i*)   इस अध्ययन से यह पता चला है कि प्रस्तावित मॉडल ऊर्जा फलक्स (E_z) तथा पर्वतीय क्षेत्र में हर स्तर पर किसी भी प्रकार के अवरोध के क्षैतिज अवयवों से संबंधित संवेग फलक्स (τ_{zx} और τ_{zy}) की गणना कर सकता है।

(*ii*)   कुछ चयनित मामलों की गणनाओं से पता चला है कि ऊर्ध्वाधर दिषा में फलक्सेस में भिन्नताएँ होती हैं। ऊर्ध्वाधर भिन्नता ऊँचाई के अनुसार एक समान नहीं होती है। अलग–अलग मामलों में यह पवन एवं तापमान के मूल प्रवाह के ऊर्ध्वाधर रूपरेखा पर निर्भर करता है तथापि सभी मामलों में पवन के मूल प्रवाह में ऊर्ध्वाधर अवयव (जो दीर्घवृत्ताकार अवरोधक के दीर्घ कटक अक्ष के समानान्तर होता है) देखा गया है।

(*iii*)   पष्चिमी घाट में '*V*' अवयव की अनुपस्थिति में संवेग फलक्स (τ_{zx}) ऊर्ध्वाधर दिषा में स्थिर होता है। कुछ स्तरों में अन्य फलक्सेस ऊर्ध्वाधर में स्थिर में होते हैं। यह अवयव मौजूद है या नहीं, इसका पता लगाने के लिए एक उपरितन स्तर का पता लगाया गया है जहाँ सभी ऊर्ध्वाधर फलक्सेस अनपसारी होते हैं।

(*iv*)   खासी जयंतिया की पहाड़ियों में '*V*' अवयव की अनुपस्थिति में τ_{zx} और τ_{zy} दोनों अवयव ऊर्ध्वाधर में स्थिर होते हैं। '*V*' अवयव की उपस्थिति τ_{zx} और τ_{zy} को प्रसारी ∕ अपसारी बनाता है।

ABSTRACT. A linear dynamical model for airflow across a three-dimensional meso-scale elliptical barrier has been used to parameterize the vertical energy flux (E_z) and the horizontal components of momentum flux (τ_{zx} and τ_{zy}) associated with orographically excited internal gravity waves (IGW) in a baroclinic background flow. This model can be used for an arbitrary orographic barrier, although in the present study an elliptical barrier has been considered. Realistic vertical variations in the stability have been incorporated in the model. The solution of model has been obtained quasi-numerically for some selected cases near the Indian mountains [The Western Ghats (WG) and the Khasi-Jayantia (KJ) hills].

(*i*)   Study shows that the proposed model can compute the energy flux (E_z) and the horizontal components of momentum flux (τ_{zx} and τ_{zy}) associated with orographically excited gravity waves at each level for any barrier.

(*ii*)   Computations for the selected cases shows that the fluxes vary in the vertical. The vertical variation is not uniform with height. It depends on the vertical profiles of the wind and temperature of basic flow for respective cases. However,

the influence of the '*V*' component (parallel to major ridge axis of elliptical barrier) of basic wind has been observed in all cases.

(*iii*)   For the WG, τ_{zx} is invariant in the vertical in absence of '*V*' component. Other fluxes are invariant in the vertical in some layers. Whether this component is present or not, an upper layer is found where all the vertical fluxes are non-divergent.

(*iv*)   For the KJ hills, in absence of '*V*' component τ_{zx} and τ_{zy} both are invariant in the vertical, presence of '*V*' component makes τ_{zx} and τ_{zy} divergent/convergent.

   Key words – Orographic gravity wave, Momentum flux.

1.   Introduction

   We know that, when a stably stratified air-stream flows across an orographic barrier, gravity waves are excited which propagate upwards under certain conditions of thermal stability and airflow stratification. These orographic gravity waves can transport momentum from a stably stratified airstreams to the earth's surface in response to a net pressure drop between the windward and lee slopes of the barrier. It is also known that these gravity waves are also capable of transporting energy from surface to the mean flow at great height. It is also believed that the continuous extraction of momentum from the mean flow is one of the possible causes for breaking of gravity waves. But this transport of momentum or energy by orographic gravity waves is a sub-grid scale phenomenon, yet its impact on large-scale motion is substantial. So the parameterization of these sub-grid scale fluxes is important in the numerical weather prediction models.

   Sawyar (1959) first pointed out the relative importance of this momentum loss of the mean flow due to continuous extraction of momentum from it by the orographic gravity waves. He examined the case of a two-dimensional (2-D) flow over a bell-shaped obstacle with half width (a) 2 km and height (b) 300 m and determined that the typical value of wave momentum flux is of the order 1-10 dynes/cm^2.

   Eliassen and Palm (1961) showed that for 2-D linear gravity waves, the vertical flux of horizontal momentum, resulting from waves, is independent of height when the waves are steady and non-dissipative.

   Bluemen (1965) noted that the magnitude of the wave drag is sensible to the vertical wavelength. He also showed that the maximum value of the drag is attained when the vertical wavelength is twice the maximum height of the mountain.

   Bretherton (1969) reviewed the theories concerning the propagation of internal gravity waves (IGW) in a horizontally uniform shear flow. His computations showed that for a 19m/s gradient wind over hilly terrain in north Welsh, the wave drag amounted to 4 dyne/cm², of which 3 dyne/cm² probably acted on the atmosphere above 20 km.

   Lilly (1972) reported that "From aircraft traverses through moderate amplitude waves in the Front Range we have commonly obtained direct stress measurements of between 5 and 10 dyne/cm^2 in the troposphere averaged over horizontal distances of 100-200 km."

   Smith (1978) determined the pressure drag on the Blue-ridge Mountain in the central Appalachians. During the first two weeks of January 1974 he observed several periods with significant wave drag with pressure differences typically of the order of 50 N/m² across the ridge.

   Palmer *et al.* (1986) has pointed out the general westerly bias of the global general circulation models (GCM). They also pointed out that one way to reduce this general westerly bias is to incorporate the gravity wave drag parameterization scheme in the GCM. Gravity wave drag parameterization scheme proposed by Palmer *et al.* (1986), McFarlane (1987) has reduced the westerly bias mainly in stratosphere.

   Recently, lee waves have drawn the new attention from the viewpoint of the atmospheric momentum budged. Iwasaki *et al.* (1989) introduced a new type of gravity wave drag parameterization scheme to improve the tropospheric westerly bias by including the effects of these tropospheric-trapped lee waves.

   Duran (1992), using a simple 2-D model, showed the importance of non-hydrostatic trapped lee waves in the troposphere.

   Satomura and Bougeault (1994) used a 2-D, non-hydrostatic, compressible model to simulate the airflow over the Pyrenees in connection with two lee wave events during PYREX experiment. In both cases, the simulated
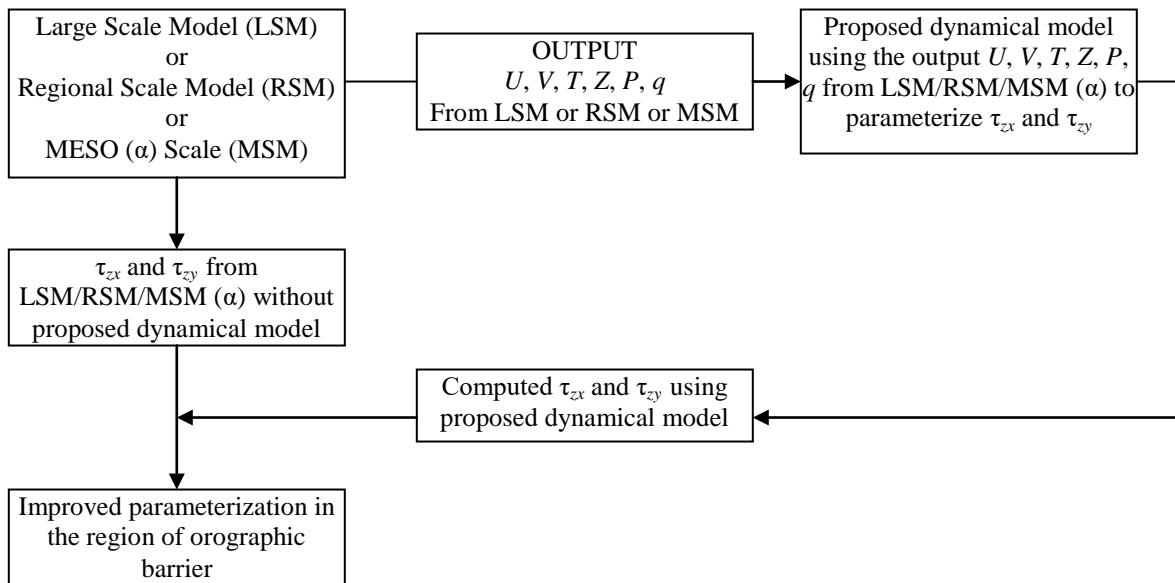
Fig. 1. Schematic diagram to show how the proposed dynamical model can be incorporated in a large scale model to improve the parameterization of vertical flux of eddy energy/horizontal momentum

downward momentum fluxes agree well with the observed fluxes around 4 km height. The simulated fluxes in their study were almost constant with height. The over estimation of simulated momentum flux in the upper half of the atmosphere was suggested to be due to the time evolution of the mean wind and the lateral momentum flux divergence found in the atmosphere.

Vosper and Mobbs (1998) showed that for steady waves, in the absence of dissipation, the vertical fluxes of both the components of horizontal momentum are constant with height.

In India, studies on orographically excited internal gravity wave have done by Das (1964), Sarker (1965), De (1971, 1973), Sarker et al. (1978), Sinha Ray (1988), Kumar et al. (1995).These studies mainly aimed at the computation of wavelength and perturbation streamline displacement, vertical velocity associated with orographically excited internal gravity wave. Dutta (2001) studied momentum/energy flux associated with mountain wave across Mumbai-Pune section of the Western Ghats in an idealized air stream. He showed that both the fluxes were independent of height and the half width of the bell shaped part of the barrier. Further it was shown that the plateau portion of the section does not contribute to the above fluxes.

In a recent study by Wells et al. (2005), the impact of rotation on the orographic drag due to flow across and around a wide mountain have been investigated. In their study, a series of idealized model experiments with a larger range of ridge lengths were performed. Implications of the results obtained for NWP parametrizations of sub-grid-scale orographic drag have been discussed.

Dutta and Naresh (2005) studied momentum and energy flux associated with mountain wave across the Assam-Burma hills. Their study shows that a long valley acts as a source in the atmospheric momentum budget and a sink in the energy budget. In these studies the vertical variation of wind and stability were not considered.

Smith et al. (2006) investigated the behaviour of the resolved Alpine pressure drag with model horizontal resolution using seven mountain wave case-studies from the Mesoscale Alpine Programme (MAP). Three independent modelling systems in their study showed that the magnitude of the resolved surface pressure drag increased monotonically as the horizontal model resolution increased from 125 km down to a few kilometres. They have also shown that a substantial proportion of the drag still need to be parameterized in the next generation of mesoscale models, with horizontal resolutions of about 5 km.

It appears from the foregoing discussions that, although there are some studies on the parameterization of momentum and energy flux associated with orographically excited internal gravity waves with realistic vertical profile of background wind and stability, hardly any such study has been done in India.

Objective of the present study is to propose a dynamical model for parameterizing energy flux and momentum fluxes associated with IGW across a 3-D mesoscale orographic barrier. In Fig. 1, schematically it has been shown how this proposed dynamical model can be used in a large scale/regional scale/meso(α) scale model for a better parameterization of momentum/energy flux in a region near a meso-scale barrier.

2. Data

Radio sonde data on selected dates of Santacruz and Agartala have been used to study near the WG region and the KJ hills respectively, because these two stations are located at far upstream distance with respect to westerly basic flow across the WG and with respect to southerly basic flow across the KJ hills. These data have been collected from the Archival of India Meteorological Department.

3. Model

The dynamical model used in this study is identical to Dutta (2005, 2007) where following assumptions considered:

(*i*) Steady state flow

(*ii*) Non-hydrostatic

(*iii*) Adiabatic basic flow (Dry or moist)

(*iv*) Laminar

(*v*) Boussinesq

Following Dutta (2005, 2007), the linearised governing equations, under the above assumptions, are subjected to double Fourier transformation and then from the transformed equations $\tilde{u}, \tilde{v}, \tilde{p}, \tilde{\theta}$ are eliminated to obtain the following vertical structure equation

$$\frac{\partial^2 \tilde{w}_1}{\partial z^2} + \left\{ f(k,l,z) - \kappa^2 \right\} \tilde{w}_1 = 0 \qquad (1)$$

where,

$$\tilde{w}(k,l,z) = \sqrt{\frac{\rho_0(0)}{\rho_0(z)}} \; \tilde{w}_1(k,l,z),$$

$$f(k,l,z) = \frac{N_m{}^2 \kappa^2}{\sigma^2} - \frac{1}{\sigma}\frac{d^2\sigma}{dz^2} - \frac{1}{\sigma}\frac{d\sigma}{dz}\frac{1}{\rho_0}\frac{d\rho_0}{dz}$$
$$+ \frac{1}{4\rho_0{}^2}\left(\frac{d\rho_0}{dz}\right)^2 - \frac{1}{2\rho_0}\frac{d^2\rho_0}{dz^2}$$

$$\kappa^2 = k^2 + l^2$$

$$\sigma = U k + V l$$

(k,l) = Horizontal wave number vector

$$N_m{}^2 = \frac{g}{\beta\overline{\theta_e}(1+q_s)}\frac{d\overline{\theta_e}}{dz}$$

$$\beta = 1 - \frac{Lq_s}{C_p\overline{T}}\left(\frac{\varepsilon+\gamma q_s}{\varepsilon+q_s}\right). \text{ Detail derivations for the}$$

expressions of $\beta, N_m{}^2$ are available in Dutta (2007). The meanings of different symbols have been given in appendix.

The Eqn. (1) is solved using the following boundary conditions:

(*i*) At the lower boundary, *i.e.*, at the surface ($z = 0$) airflow is tangential to the ground surface, *i.e.*, $w'(x,y,0) = U(0)\dfrac{\partial \eta'(x,y,0)}{\partial x} + V(0)\dfrac{\partial \eta'(x,y,0)}{\partial y}$, where, $\eta'(x,y,0)$ is the vertical streamline displacement at $z = 0$. Since at the lower boundary ($z = 0$) the streamline pattern follows the terrain, hence $\eta'(x,y,0) = h(x,y)$, where $z = h(x,y)$ is the three-dimensional profile of the orographic barrier.

So, $\tilde{w}(k,l,0) = \tilde{w}_1(k,l,0) = i\sigma(k,l,0)\tilde{h}(k,l)$

In this study the three dimensional profile has been approximated by an ellipsoid, given by

$$h(x,y) = \frac{H}{1+\left(\dfrac{x}{a}\right)^2+\left(\dfrac{y}{b}\right)^2}$$

Here, *x*-axis is parallel to the minor ridge axis and *y*-axis is parallel to the major ridge axis of the elliptical barrier. For the WG, major axis being north-south oriented, *x*-axis points towards east, *y*-axis points towards

north and z-axis points vertically upwards. For the KJ hills, major axis being east-west oriented, x-axis points towards north, y-axis points towards west and z-axis points vertically upwards. Thus for the WG, u-component of wind is towards east (westerly), v-omponent towards north (southerly) and for the KJ hills, u-component of wind is towards north (southerly), v-component towards west (easterly).

With above expression for $h(x, y)$, we have, $\tilde{h}(k,l) = 2\pi ab H K_0(\sqrt{a^2k^2 + b^2l^2})$, K_0 being the Bessel function of second kind (Dutta *et al.*, 2002). Although we have taken an analytical profile for the barrier in the present study, it is possible to find out the Fourier transform of $h(x, y)$ numerically, in case $h(x, y)$ is given at discrete grid points.

For the Western-Ghats, $H = 0.77$ km, $a = 18$ km, $b = 45$ km (Dutta 2005) and for the Khasi-Jayantia hills $H = 1.6$ km, $a = 25$ km, $b = 62.5$ km (De, 1973).

(*ii*) The approximate solution of Eqn. (1) in the region of $f(k, l, z) \approx 0$ is of the form

$$\tilde{w}_1(k,l,z) \propto e^{-\kappa z} \qquad (2)$$

c being arbitrary constant. Since the pressure, vertical velocity are continuous functions of z, therefore, $\tilde{w}_1, \dfrac{\partial \tilde{w}_1}{\partial z}$ are also continuous functions of z. So, in the region where

$$f(k, l, z) \approx 0, \ \frac{\partial \tilde{w}_1}{\partial z} = -\kappa \tilde{w}_1 \qquad (3)$$

Equations (2) and (3) provide upper boundary conditions.

(*iii*) Lateral boundary conditions are periodic.

Then using the above boundary conditions and following Dutta (2005), Eqn. (1) is solved quasi numerically. The solution for $\tilde{w}_1(k,l,z)$ is given by

$$\tilde{w}_1(k,l,z) = i\sigma(k,l,0)\tilde{h}(k,l)\frac{\psi(k,l,z)}{\psi(k,l,0)} \qquad (4)$$

and hence,

$$\tilde{w}(k,l,z) = \sqrt{\frac{\rho_0(0)}{\rho_0(z)}} i\sigma(k,l,0)\tilde{h}(k,l)\frac{\psi(k,l,z)}{\psi(k,l,0)} \qquad (5)$$

where $\psi(k,l,z)$ is an arbitrary function satisfying equations (1), (2) and (3), and also it's value above the upper boundary is 1. Following Dutta (2005), $\psi(k,l,z)$ has been computed numerically at different discrete vertical levels, separated by a distance $d = 0.25$ km, for a given wave number vector (k,l).

Again it can be shown that

$$\tilde{p}(k,l,z) = \frac{i\rho_0(z)}{\kappa^2}\left\{\frac{d\sigma}{dz}\tilde{w}(k,l,z) - \sigma\frac{\partial \tilde{w}}{\partial z}\right\} \qquad (6)$$

$$\tilde{u}(k,l,z) = \frac{i\left[\tilde{w}(k,l,z)\dfrac{dU}{dz} - \dfrac{k}{\kappa^2}\left\{\tilde{w}(k,l,z)\dfrac{d\sigma}{dz} - \sigma\dfrac{\partial\tilde{w}}{\partial z}\right\}\right]}{\sigma} \qquad (7)$$

$$\tilde{v}(k,l,z) = \frac{i\left[\tilde{w}(k,l,z)\dfrac{dV}{dz} - \dfrac{l}{\kappa^2}\left\{\tilde{w}(k,l,z)\dfrac{d\sigma}{dz} - \sigma\dfrac{\partial\tilde{w}}{\partial z}\right\}\right]}{\sigma} \qquad (8)$$

where, $\sigma(k,l,z) = kU(z) + lV(z)$ is the component of basic horizontal wind (U,V) along the wave number vector (k,l).

Now, from Eqn. (5) and from the vertical profile of basic state wind and temperature field, $\tilde{p}, \tilde{u}, \tilde{v}$ can be found out and also using Eqn. (5) $\tilde{w}$ can be found out at each level for a given wave number vector (k,l). By performing inverse double Fourier transformation on Eqns. (5)-(8) numerically, we obtain w', p', u', v' at each horizontal grid point (5 km apart) at each vertical level. Then the two horizontal components of the momentum flux vector, *viz.*, $\tau_{zx} = \overline{\overline{u'w'}}$, $\tau_{zy} = \overline{\overline{v'w'}}$ and the energy flux $E_z = \overline{\overline{p'w'}}$ at any vertical level at any model horizontal grid point can be computed, where, $\overline{\overline{(\ )}}$ indicates the average over the surface area 'S' of the barrier. Below it is shown that $S = \dfrac{\pi^2(a+b)H}{2}$:

At any height, z the elliptical contour is given by $\dfrac{x^2}{\alpha^2} + \dfrac{y^2}{\beta^2} = 1$, where $\alpha^2 = a^2\left(\dfrac{H}{Z} - 1\right)$ and $\beta^2 = b^2\left(\dfrac{H}{Z} - 1\right)$. So, the area '$dS$' of a strip of thickness dz at this height is the product of dz and the perimeter of
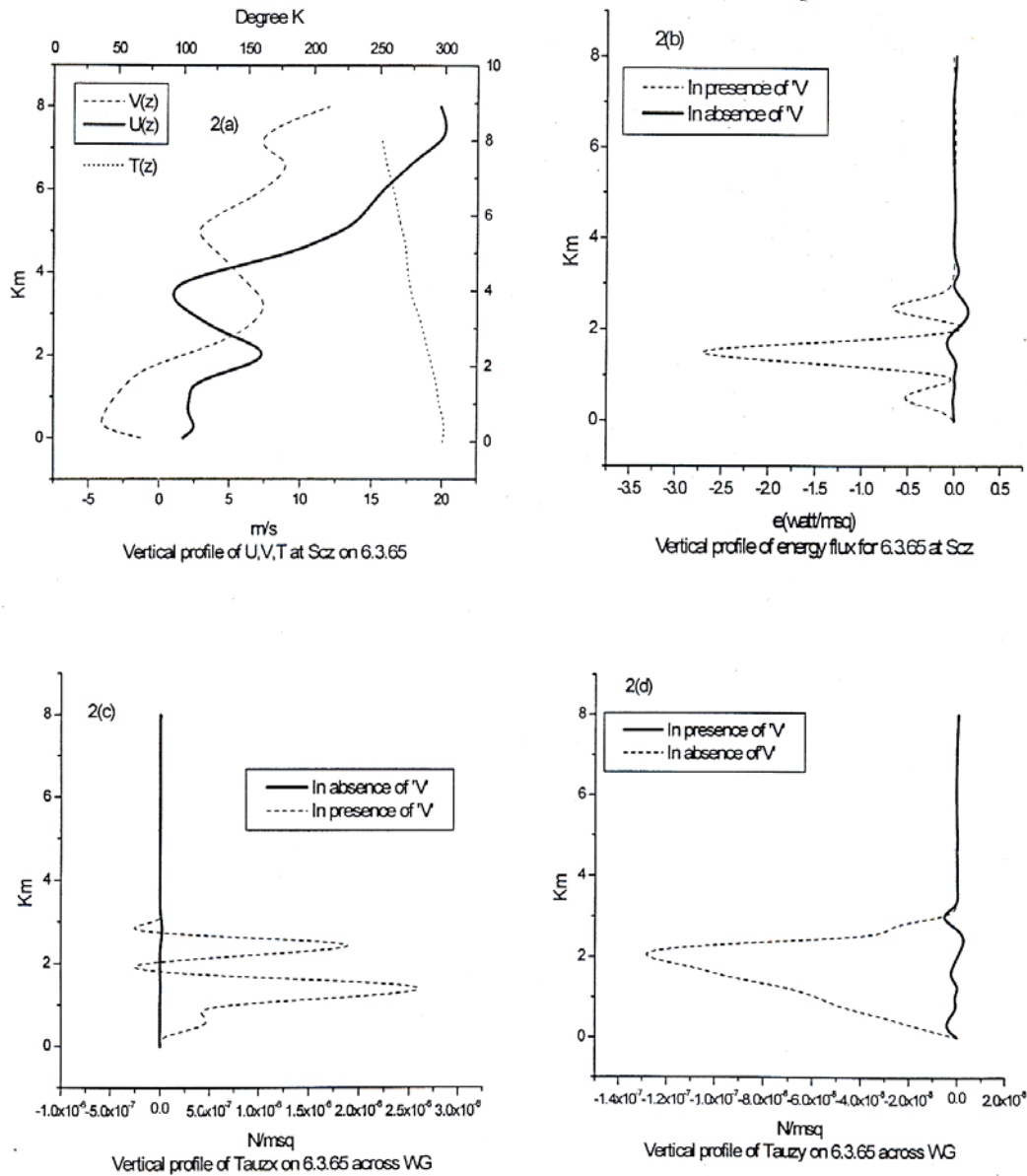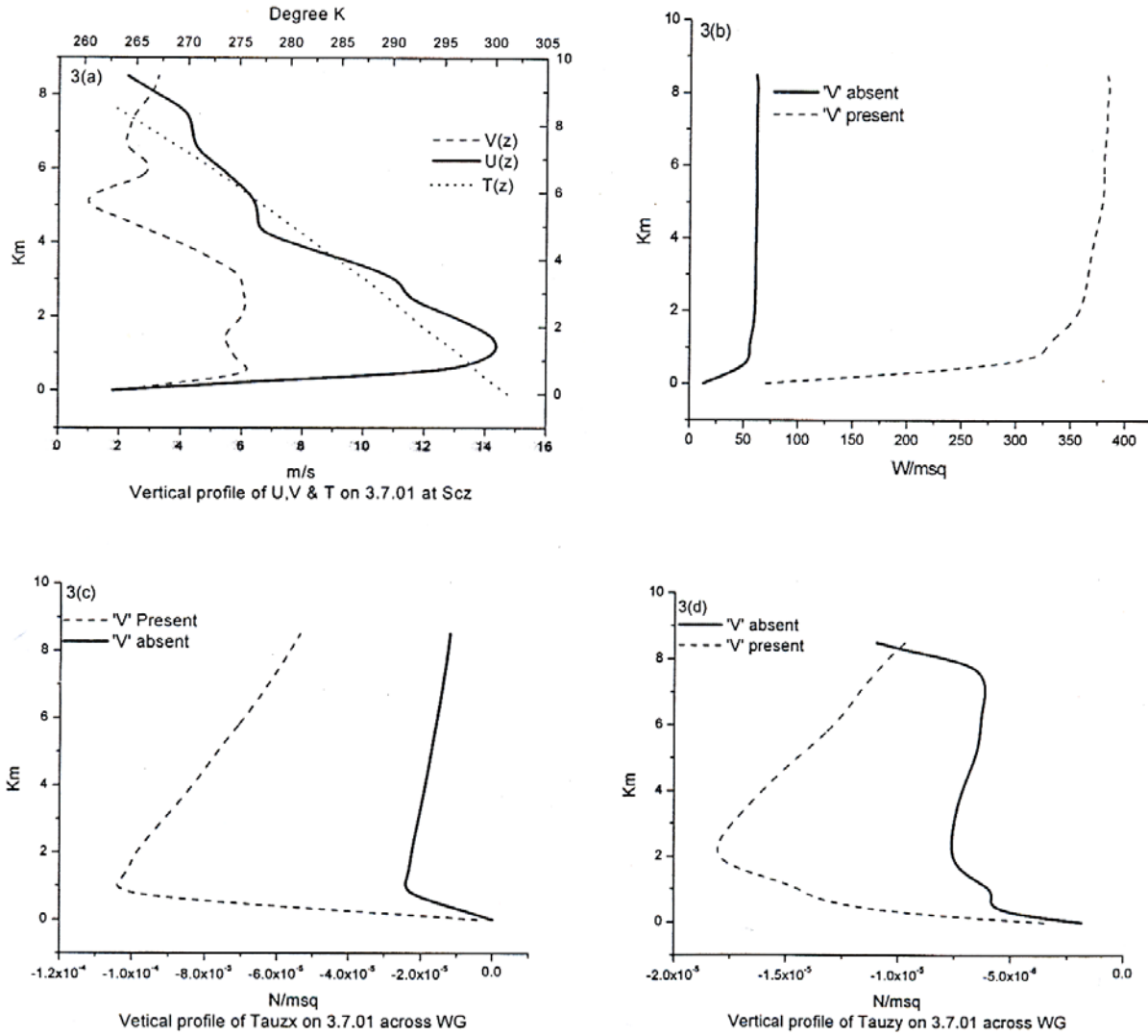
Figs. 2(a-d).   Vertical profile of (a) *U*, *V*, *T*, (b) energy flux at Santacruz, (c) westerly-momentum flux and (d) southerly-momentum flux across Western Ghat (WG) on 6 March 1965

the above ellipse is given by $dS = \pi\,(\alpha+\beta)dz$. Hence the total surface area of the barrier is

$$S = \int ds = \int_0^H \pi(\alpha+\beta)dz$$

$$= \pi(a+b)\int_0^H \left(\sqrt{\frac{H}{z}}-1\right)dz = \frac{\pi^2(a+b)H}{2}.$$

4.   Discussions

In this section some selected cases for the WG as well as for the KJ hills have been studied. Sarker (1965, 1967) showed that the air stream during winter/pre-monsoon and during the summer monsoon is favourable for the formation of lee waves across the WG. Also De (1973), Sinha Ray (1988) and Sarker *et al.* (1978) have shown that the air stream during the summer monsoon is

Figs. 3(a-d).   Vertical profile of (a) *U*, *V*, *T*, (b) energy flux at Santacruz, (c) westerly-momentum flux and (d) southerly-momentum
flux across Western Ghat (WG) on 3 July 2001

favourable for the formation of lee waves across the KJ hills. Accordingly in this section four cases have been studied, *viz*., lee wave across the WG during winter/pre-monsoon, lee wave across the WG during summer Monsoon and two lee wave cases across the KJ hills during summer monsoon.

(*i*)   For cases of lee waves across the Western Ghats (WG) during winter/pre-monsoon and summer monsoon.

Case-1 :   *For the lee wave across the WG during
winter/pre-monsoon (on 6 March 1965)*

The vertical profiles of *U*, *V* and *T* are shown in Fig. 2(a), which are based on the 0000 UTC and 1200 UTC Radio sonde data of Santacruz of 6th March 1965.

Using the above profile the vertical energy flux (E_z) and momentum fluxes (τ_{zx} and τ_{zy}) at different levels have been computed.
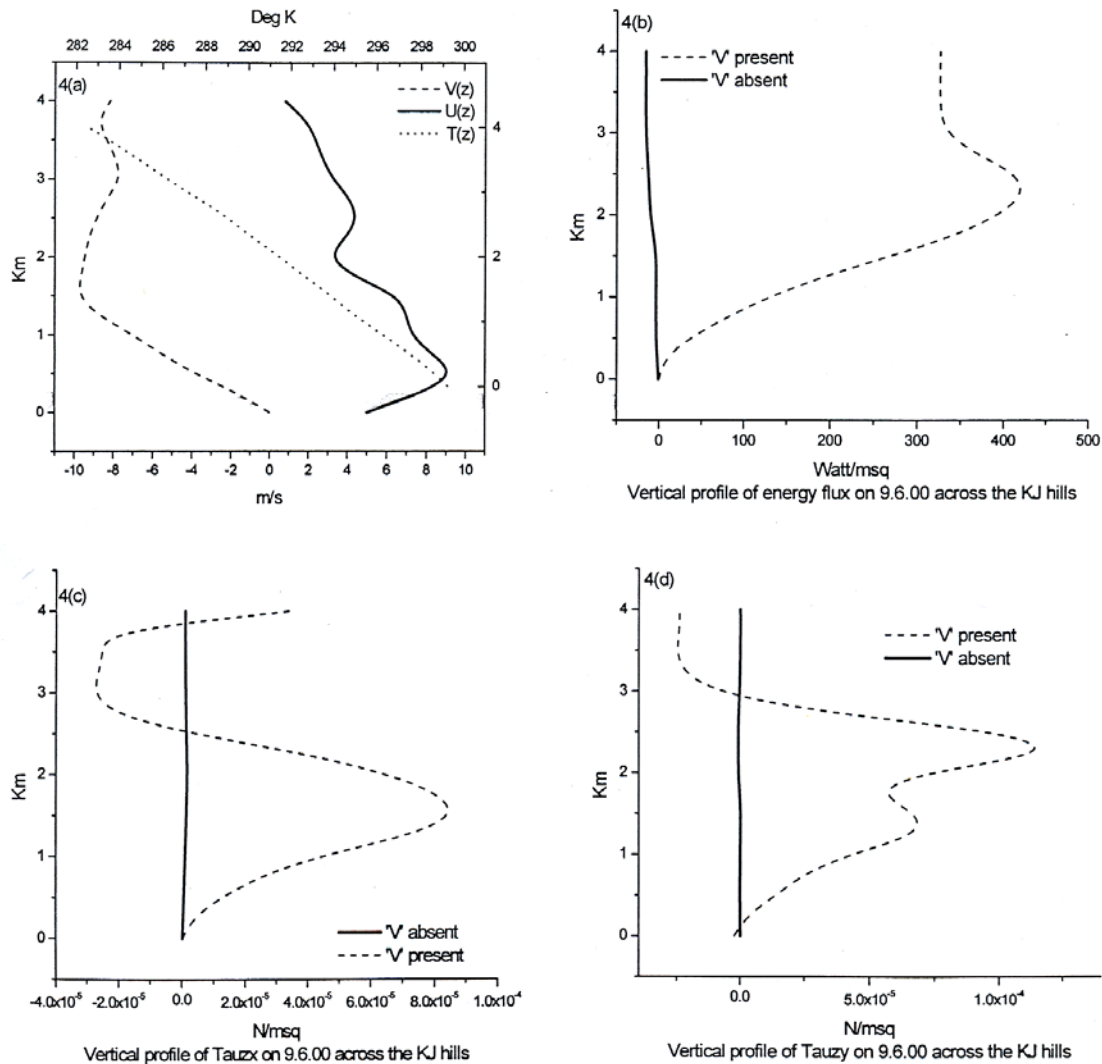
Figs. 4(a-d).   Vertical profile of (a) *U*, *V*, *T*, (b) energy flux at Khasi-Jayantia (KJ), (c) westerly-momentum flux and (d) southerly-momentum flux across the Khasi-Jayantia (KJ) on 9 June 2000

The vertical profile of energy flux (E_z) has been shown in Fig. 2(b). From this figure it can be seen that, whether '*V*' is present or not, above $z = 3.5$ km, E_z is practically invariant in the vertical. It can also be seen that it remains invariant in the vertical at lower levels up to $z = 1$ km in the absence of '*V*' component. Divergence/convergence in E_z can be seen in the layer up to $z = 3.5$ km in presence of '*V*' and in the layer from $z = 1$ km to $z = 3.5$ km, in the absence of '*V*'. It is to note

that presence of the vertical shear of the basic flow and the presence of '*V*' makes E_z vertically downward, whereas in the absence of vertical shear of basic flow it is upward.

The vertical profiles of westerly-momentum flux (τ_{zx}) and southerly-momentum flux (τ_{zy}) have been shown in Figs. 2(c&d). From theses figure it can be seen that, in the absence of '*V*', they are practically zero and invariant in the vertical. Presence of '*V*' only makes them

divergent/convergent. Vertically upward τ_{zx} can also be seen in presence of 'V', which is generally vertically downward in case of a constant 'U' and $V = 0$.

Case-2 : *For the lee wave across the WG during Southwest-monsoon (on 3 July 2001)*

The vertical profiles of   *U*, *V* and *T*, based on average of 0000 UTC and 1200 UTC Radio sonde data of Santacruz of 3rd July 2001, are shown in Fig. 3(a). Since during July the westerly airflow impinging on WG is moist, hence in this case, *T*(*z*) has been approximated by the pseudo-adiabatic line through the surface dry bulb temperature. In Dutta (2005), it has been shown that this vertical profile of wind is favourable for giving mountain wave.

The vertical profile of energy flux (E_z) in watt/msq is shown in Fig. 3(b). First it can be seen that energy flux is upward. It can also be seen that, whether 'V(mean southerly)' is present or not, E_z is divergent in the vertical up to 0.5 km and above this level it is practically non divergent.

The vertical profile of westerly-momentum flux (τ_{zx}) in N/msq is shown in Fig. 3(c). First it can be seen that, this flux is downward whether 'V' component is present or not. It can also be seen that magnitude of this flux has enhanced in presence of this component of basic flow. It is observed from this figure that τ_{zx} is convergent in a shallow layer near the surface above which it is divergent. Convergence/divergence of τ_{zx} is enhanced in presence of 'V'.

The vertical profile of southerly-momentum flux (τ_{zy}) in N/msq is shown in Fig. 3(d). Similar to τ_{zx} , this flux is also downward throughout the vertical domain. We find from this figure that irrespective of the 'V' component of basic flow, τ_{zy} is convergent in the layer from surface to 2 km, above which it is divergent. In the absence of 'V', it is again convergent in a shallow layer near the top of vertical domain.

(*ii*) For cases of lee waves across the Khasi-Jayantia hills (KJ hills) during summer monsoon:

Although in the model computation of the following cases for the KJ hills, *U* stands for southerly component and *V* stands for easterly component of basic flow, while preparing the vertical profile of fluxes care has been taken so that, as usual τ_{zx} represents vertical flux of westerly momentum and τ_{zy} represents that of southerly momentum.

Case-3 : *For the lee wave across the KJ hills during Southwest monsoon (on 9 June 2000)*

The vertical profiles of *U*, *V* and *T* are shown in Fig. 4(a), based on the 0000 UTC and 1200 UTC Radio sonde data of Agartala of 9th June 2000. In this case *V* is negative at all levels. Since during this season the southerly flow across KJ hills is neutral with respect to moist adiabatic lapse rate, hence following Sarker (1967), De (1971) here also we have approximated *T*(*z*) by the pseudo-adiabat through the surface dry bulb temperature.

The vertical profiles of E_z, τ_{zx} and τ_{zy} are shown in Figs. 4(b-d).

It is seen from Fig. 4(b) that the magnitude of E_z is one order larger than those in cases 1 and 2. It can be seen that in absence of 'V' component energy flux is non-divergent and it is almost nil throughout vertical. In presence of this component of basic flow, we find layers with divergent/convergent energy flux. Energy flux is divergent in the layer from surface to 2.5 km, above this level it is convergent upto 3 km and then it is non-divergent in the remaining vertical domain.

From Figs. 4(c&d), in absence of 'V' component, we find almost non-divergent vertical flux of both component of horizontal momentum (τ_{zx} and τ_{zy}) and also they are practically nil throughout the vertical. First of all both the fluxes are downward in the presence of this component. In presence of this component we find different layers with divergent/convergent momentum flux. We find divergent τ_{zx} in the layer from surface to 1.5 km, above this level it is convergent upto 3 km, then it is non-divergent upto about 3.5 km and then again it is divergent. τ_{zy} is found to be divergent in the layer from surface to 2.5 km, above this level it is convergent upto 3 km, then it is non-divergent.

Case-4 : *For the lee wave across the KJ hills during Southwest monsoon (on 1 August 2000)*

The vertical profiles of *U*, *V* and *T* are shown in Fig. 5(a), based on the 0000UTC and 1200UTC Radio sonde data of Agartala of 1st August 2000. Similar to previous case, in this case also *V* is negative at all levels. Following similar argument as in the previous case, here also we have approximated *T*(*z*) by the pseudo-adiabat through the surface dry bulb temperature.

The vertical profiles of E_z, τ_{zx} and τ_{zy} are shown in Figs. 5(b-d).
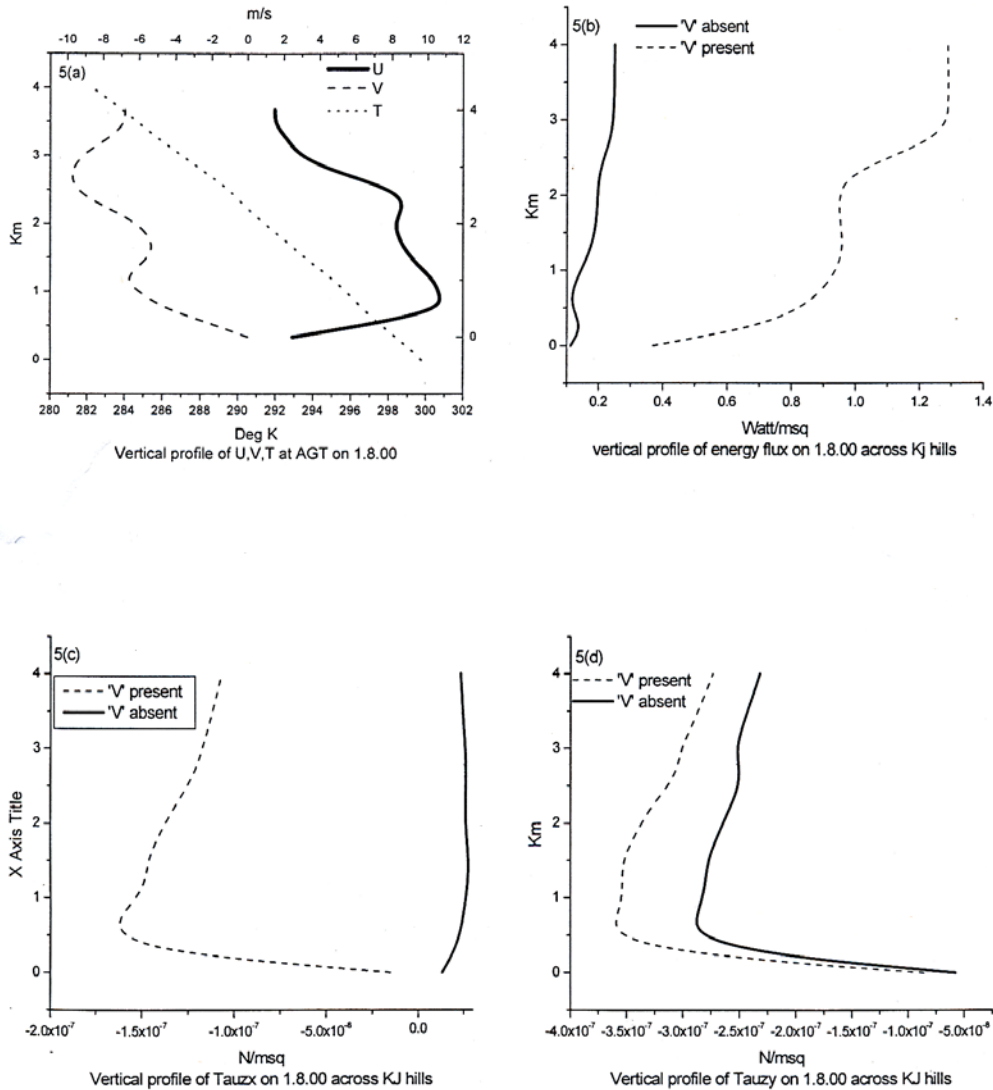
Figs. 5(a-d).   Vertical profile of (a) *U*, *V*, *T*, at Agartala, (b) energy flux across Khasi-Jayantia (KJ), (c) westerly-momentum flux and (d) southerly-momentum flux across the Khasi-Jayantia (KJ) on 1 August 2000

It is seen from Fig. 5(b) that, the presence of '*V*' component has enhanced the magnitude of E_z. In presence of this component of the basic flow, the E_z is divergent in the layer between 0 to 1 km and between 2 to 3 km. E_z is non-divergent from 1 to 2 km and from 3 to 4 km. In the absence of this component, E_z is divergent in the layer from $z = 1$ km to 3 km and non-divergent above it.

From Fig. 5(c) it is seen that τ_{zx} is upward and is nearly non-divergent in the absence of '*V*' component. In presence of this component τ_{zx} is downward and also there are layers with divergent/convergent τ_{zx}. We find

very strong convergence of τ_{zx} in the lowest layer up to about 0.5 km above which τ_{zx} is divergent.

Fig. 5(d) shows strong convergence of τ_{zy} in the lowest layer up to about 0.5 km above which it is divergent.

5.   Conclusions

(*i*)   The above model is capable of computing, the vertical energy flux (E_z) and the components of eddy

horizontal momentum flux in the direction parallel to the major ridge (τ_{zy}) and normal to it (τ_{zx}), at all levels.

(*ii*) Computation shows that all the fluxes vary in the vertical. The vertical variation is not uniform with height. In some layers fluxes are upward and somewhere it is downward. But in most cases energy flux is upward and momentum fluxes downward. Direction of fluxes depends on the vertical profiles of the wind and temperature of basic flow for respective cases.

(*iii*) However, the influence of the 'V' component of basic wind has been observed in all cases. This component makes the energy flux or momentum flux divergent/convergent in the vertical in most of the cases.

(*iv*) For the WG, τ_{zx} is invariant in the vertical in absence of 'V' component. Other fluxes are invariant in the vertical in some layers. For the WG, whether this component is present or not, an upper layer is found where all the vertical fluxes are non-divergent.

(*v*) From the cases studied it is found that the magnitude of energy flux across the KJ hills is one order more than that across the WG.

(*vi*) For the KJ hills, in absence of 'V' component τ_{zx} is non-divergent, presence of 'V' component makes it divergent/convergent.

Acknowledgements

References

Bluemen, W., 1965, "A random model of momentum flux by mountain waves", *Geofys. Publ.*, **26**, 1-33.

Bretherton, F. P., 1969 "Momentum transport by gravity waves", *Quart. J. R. Met. Soc.*, **95**, 213-243.

Das, P. K., 1964, "Lee waves associated with a large circular mountain", *Indian J. Met. & Geophys.*, **15**, 547-554.

De, U. S., 1971, "Mountain waves over northeast India and neighbouring regions", *Indian J. Met. & Geophys.*, **22**, 361-364.

De, U. S., 1973, "Some studies of mountain waves", Ph. D. Thesis submitted to Banaras Hindu University.

Duran, D. R., 1992, "Orographic wave drag on the middle and lower troposphere", The importance of trapped waves, Physical processes in atmospheric models, 1992, Collected lectures, Edited by D. R. Sikka and S. S. Singh, Published by Willey Eastern Publishing Co., 319-332.

Dutta, S. N., 2001, "Momentum flux, energy flux and pressure drag associated with mountain wave across Western Ghat", *Mausam*, **52**, 2, 325-332.

Dutta, S. N., Maiti, M. and De, U. S., 2002, "Waves to the lee of a meso-scale 3-dimensional elliptical orographic barrier", *Meteorology and Atmospheric Physics*, **81**, 3-4, 219-235.

Dutta, Somenath and Kumar, Naresh, 2005, "Parameterization of momentum and energy flux associated with mountain wave across the Assam- Burma hills", *Mausam*, **56**, 3, 527-534.

Dutta, S., 2005, "Effect of static stability on the pattern of three-dimensional baroclinic lee wave across a meso-scale elliptical barrier", *Meteorology and Atmospheric Physics*, **90**, 139-152.

Dutta, S., 2007, "A meso-scale three-dimensional dynamical model of orographic rainfall", *Meteorology and Atmospheric Physics*, **95**, 1-2, 1-14.

Eliassen, A. and Palm, E., 1961, "On the transfer of energy in stationary mountain waves", *Geophys. publ.*, **22**, 3, 1-23.

Iwasaki, T. S., Yamada, S. and Tada, K., 1989, "A parameterization scheme of orographic gravity wave drag with two different vertical partitioning. Part-I : Impacts on medium range forecasts", *J. Met. Soc. Japan*, **67**, 11-27.

Kumar, P., Singh, M. P., Padmanabhan, N. and Natarajan, N., 1995, "Effect of latent heat release on mountain waves in a sheared flow", *Mausam*, **46**, 111-126.

Lilly, D. K., 1972, "Wave momentum flux – A GARP problem", *Bull. Amer. Met. Soc.*, **53**, 17-23.

McFarlane, N. A., 1987, "The effect of orographically excited gravity wave drag on the general circulation of the lower Stratosphere and Troposphere", *J. Atmos. Sci.*, **44**, 1775-1800.

Palmer, T. N., Shutts, G. J. and Swinbank, R., 1986, "Alleviation of a systematic westerly bias in general circulation and numerical weather prediction models through an orographic gravity wave drag parameterization", *Quart. J. R. Met. Soc.*, **112**, 1001-1039.

Sarker, R. P., 1965, "A Theoretical study of Mountain waves on Western Ghats", *Indian J. Met. & Geophys.*, **16**, 4, 565-584.

Sarker, R. P., 1967, "Some modifications in a Dynamical model of orographic rainfall", *Mon. Wea. Rev.*, **95**, 673-684.

Sarker, R. P., Sinha Ray, K. C. and De, U. S., 1978, "Dynamics of orographic rainfall", *Indian J. Met. & Geophys.*, **29**, p348.

Satomura, T. and Bougeault, P., 1994, "Numerical simulation of lee wave events over the Pyrenees", *J. Met. Soc. Japan*, **72**, 2, 173-195.

Sawyar, J. S., 1959, "The introduction of the effects of topography into methods of numerical forecasting", *Quart. J. R. Met. Soc.*, **85**, 31-43.

Sinha Ray, K. C., 1988, "Some studies on effects of Orography on airflow and rainfall", Ph.D. thesis, University of Pune, India.

Smith, R. B., 1978, "A measurement of mountain drag", *Journal of the Atmospheric Science*, **35**, 9, 1644-1654.

Smith, S. A., Doyle, J. D., Brown, A. R. and Webster, S., 2006 (Part A), "Sensitivity of resolved mountain drag to model resolution for MAP case-studies", *Quart. J. R. Met. Soc.*, **132**, 1467-1487.

Vosper, S. B. and Mobbs, S. D., 1998, "Momentum flux due to three dimensional gravity waves : Implications for measurements and numerical modeling", *Quart. J. R. Met. Soc.*, **124**, 2755-2769.

Wells, Helen, Webster, Stuart and Brown, Andrew, 2005 (Part B), "The effect of rotation on the pressure drag force produced by flow around long mountain ridges", *Quart. J. R. Met. Soc.*, **131**, 1321-1338.

Appendix

List of symbols

Symbol	Meaning
x	Horizontal co-ordinate in the direction normal to the major ridge of the elliptical barrier.
y	Horizontal co-ordinate in the direction parallel to the major ridge of the elliptical barrier.
z	Vertical co-ordinate pointing towards local vertical.
U	Horizontal component of basic flow along x-axis.
V	Horizontal component of basic flow along y-axis.
u'	Component of perturbation wind along x-axis.
v'	Component of perturbation wind along y-axis.
w'	Component of perturbation wind along z-axis.
$\rho_0(z)$	Density of basic flow at level 'z'.
q_s	Basic state saturated mixing ratio of water vapour at level 'z'.
$\bar{\theta}_e$	Equivalent potential temperature of basic flow at level 'z'.
p'	Perturbation pressure.
ρ'	Perturbation density.
θ_e'	Perturbation equivalent potential temperature
$\tilde{u}, \tilde{v}, \tilde{w}, \tilde{p}, \tilde{\rho}, \tilde{\theta}$	2-D Fourier transform of u', v', w', p', ρ' and θ' respectively.
$\bar{T}$	Absolute temperature of the basic flow.
k	Horizontal wave number along x-axis.
l	Horizontal wave number along y-axis
$\kappa = \sqrt{k^2 + l^2}$	Magnitude of horizontal wave number vector.
C_p, C_v	Specific heats of gas at constant pressure and at constant volume respectively.
γ	C_p/C_v
$z = h(x, y)$	Analytical expression for 3-D elliptical barrier.
$\tilde{h}(k, l)$	2-D Fourier transform of $h(x, y)$
$\psi(k, l, z)$	Arbitrarily defined function, satisfying the same upper boundary condition as $\tilde{w}_1(k, l, z)$.
$\sigma(k, l, z) = kU(z) + lV(z)$	Component of the basic flow along the wave number vector (k, l).

———————